J. Electroanal. Chem., 345 (1993) 351–362
Elsevier Sequoia S.A., Lausanne
JEC 02359

Unexpected redox rectification by an electrochemically prepared iridium oxide electrode/aqueous acid interface

Christopher S. Johnson and Joseph T. Hupp *
Department of Chemistry, Northwestern University, Evanston, IL 60208 (USA)

(Received 4 June 1992; in revised form 2 July 1992)

Abstract

In highly acidic aqueous solutions, electrochemically prepared iridium oxide films behave as steady-state insulators and transient rectifiers towards the $Ru(NH_3)_6^{3+/2+}$ redox couple. In less acidic solutions the films show only partial transient rectification or else fully reversible transient behavior, together with Koutecky–Levich-type steady-state behavior. Experimental studies, as a function of $Ru(NH_3)_6^{3+}$ concentration, solution pH, film thickness, voltammetric sweep rate and electrode rotation rate, show that these unusual phenomena are related to: (1) transient uptake of $Ru(NH_3)_6^{3+}$, apparently in place of H^+, during film-based Ir(IV/III) cycling; (2) Donnan exclusion of $Ru(NH_3)_6^{3+}$ from the reduced film under steady-state conditions; and/or (3) film-based diffusional inhibition of $Ru(NH_3)_6^{3+}$ reduction.

INTRODUCTION

Electrochemically prepared iridium oxide films have attracted attention because of their electrochromic properties [1–4], their superiority as water oxidation catalysts [5–8], and their intrinsic redox chemistry [9–20]. We have been interested in the last feature from the point of view of unusual interfacial reaction pathways (e.g. surface redox-mediated oxidations of solution-phase species, electrochemical hydride transfers or atom transfers, etc.). We reasoned that the known electrochemical accessibility of iridium (film) oxidation states III, IV and, apparently, VI [7,8], and the coupling of these to proton uptake and release [9–20], would provide a chemical basis for unusual interfacial reactivity. Indeed, unpublished preliminary studies of both methanol and ascorbate electro-oxidation at iridium oxide have suggested the occurrence of unconventional reaction mechanisms.

* To whom correspondence should be addressed.

For irreversible organic oxidations the overall electrochemical behavior is fairly complex, reflecting both the multielectron nature of the solution-phase chemical transformation (e.g. methanol to formate or CO_2, etc.) and the inherent electrochemical complexity of the film itself. In order to learn more about the latter, we decided to examine a very simple inorganic reaction: the one-electron reduction and re-oxidation of the ruthenium(III) hexaammine cation. Note that $Ru(NH_3)_6^{3+}$ is substitutionally inert and that its formal reduction potential (E_f) is close to the potential for the film-based iridium (IV/III) couple; note further that the iridium couple is pH dependent; for example [2]

$$Ir(OH)_3 \rightleftarrows Ir(O)(OH)_2 + H^+ + e^-(\text{metal electrode}) \quad (1)$$

The proximity of the two redox potentials was deemed interesting because the iridium(III) oxide is nominally insulating, while the Ir(IV) form is an electronic conductor [13]. We were hopeful, therefore, that $Ru(NH_3)_6^{3+}$ could serve as a simple probe of the potential-dependent (pH-dependent) electrochemical conductivity of the oxide film (i.e. the ability of the film to deliver oxidizing or reducing equivalents to solution species).

Our preliminary observations point to much more interesting behavior. For example, at pH 2 or higher, seemingly simple, reversible $Ru(NH_3)_6^{3+/2+}$ cyclic voltammetry is observed. At pH 0, however, transient rectifying behavior is seen (i.e. only reduction is seen by cyclic voltammetry; see also ref. 21). Further studies indicate that this unusual effect is related microscopically to the uptake of cations during film reduction. Finally, steady-state experiments, as both a function of pH and film thickness, show that electrochemical reduction actually occurs at the underlying metal—the film itself functioning (depending on pH) as either a diffusional barrier or a Donnan exclusion membrane.

The purpose of this report is to outline in brief form our experimental observations and to suggest a mechanism for the unusual reactivity patterns.

EXPERIMENTAL

Aqueous sulfuric acid (1.0 M) and trifluoromethanesulfonic (triflic) acid (0.1 and 0.01 M) solutions were prepared from the concentrated acids (Mallinckrodt and Alfa Chemicals, respectively) by using distilled water which had additionally been passed through a Barnsted Millipore NANO-pure purification system. The ionic strength of the most dilute triflic acid solution (pH 2) was adjusted to $\mu = 0.1$ M by addition of 0.09 M sodium triflate which had been prepared via neutralization of triflic acid with sodium bicarbonate. The pH values of the other solutions were maintained with buffers as follows: acetic acid/acetate (pH 3.8), sodium hydrogen phosphate/disodium hydrogen phosphate (pH 7.0) and sodium borate (pH 9.7). $[Ru(NH_3)_6]Cl_3$ and $[Ru(NH_3)_6]Cl_2$ were both supplied by Aldrich. Lanthanum perchlorate (hydrated) was obtained from GFS Chemicals. The iridium working electrode (approx. 1.0 mm diameter, 99.9% Aesar) was constructed as a rotating disk (Hysol epoxy and teflon shroud) and designed to fit a Pine

AFMSRX rotator. To remove prior films, the electrode was lightly sanded (moist 1200 grit SiC paper) before each new experiment. It was then polished with successively smaller particles of alumina (to 0.05 μm). In addition, to remove loose alumina particles, the electrode was sonicated briefly (distilled water) following each polishing step.

Both cyclic and rotating disk voltammetry were performed in conventional two-compartment cells featuring a platinum counter electrode and a saturated calomel reference electrode (SCE). All potentials are reported versus the SCE. Control of potentials was provided by either a Pine Instruments AFRDE4 or a Princeton Applied Research 264A potentiostat. Experiments were recorded with a Houston Omnigraphics 2000 X–Y recorder.

RESULTS AND DISCUSSION

Oxide film growth and voltammetric behavior

Consistent with earlier reports [1–20,22–26] repetitive scanning of the potential of a well-polished electrode between +1.26 and −0.24 V vs. SCE in 1 M H_2SO_4 results in steady growth of an electroactive oxide film, as suggested by Fig. 1. Typical cycling conditions (5 min at 5 V/s) yielded films containing $\sim 5 \times 10^{-8}$ mol/cm^2 electroactive iridium, based on integration of the Ir(III/IV) wave at approx. +0.7 V. Other voltammetric features (Fig. 1) included: (1) small hydrogen adsorption peaks (underlying iridium metal) near −0.1 to +0.2 V; (2) a region of very little current flow (insulating Ir(III)) encompassing −0.05 to +0.4 V; (3) an Ir(III/IV) redox wave centered at about +0.7 V; (4) a broad structureless

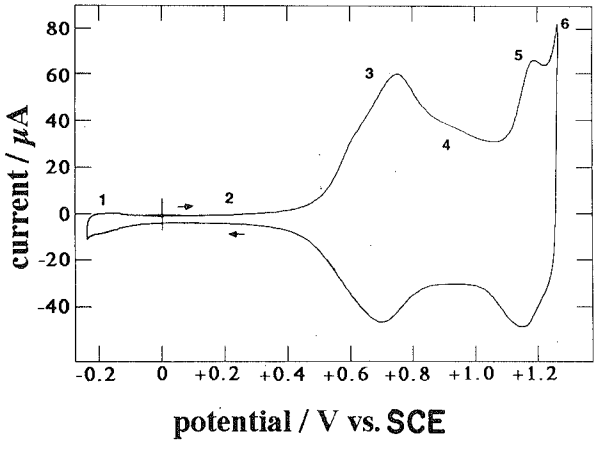

Fig. 1. Cyclic voltammogram (100 mV/s) of a hydrous iridium oxide film in 1.0 M H_2SO_4 solution. The film was grown on iridium metal by potential cycling (5 V/s) between −0.24 and +1.26 V vs. SCE for 5 min (500 cycles). See text for a description of the characteristic features of the voltammogram.

charging region beginning near +0.8 V; (5) a comparatively narrow set of peaks centered at +1.1 V; and (6) a sharply increasing anodic current associated with the onset of water oxidation near +1.2 V. The exact nature of features 4 and 5 is somewhat controversial [12,13,15]. Assignments which we find appealing and internally consistent, however, are ones which ascribe feature 4 to the gradual oxidation (i.e. non-integral charging, or metal–oxygen–dπ band depletion) of a material initially prepared (+0.8 V) in oxidation state IV, and feature 5 to the discrete two-electron oxidation of specific (perhaps oligomeric?) iridium (IV) centers. (Thus, two forms of iridium (IV) oxide are postulated [12,19,20].)

Integration of feature 5 (using feature 4 as a base line) suggests that it comprises a small minority (approx. 6–20%) of the total available metal oxide, where the variability in the estimate reflects both film preparation conditions and film history. (For example, films grown at 100 mV/s exhibit proportionately less of feature 5 than those grown at 5 V/s, while aged films exhibit preferential loss of this feature. Thermally prepared films [27], on the other hand, seem to lack this feature altogether.)

Transient redox studies

Figure 2a shows the cyclic voltammetric response of 10 mM $Ru(NH_3)_6^{3+}$ at pH 2 at an iridium oxide surface. A more-or-less ideal, reversible wave is observed,

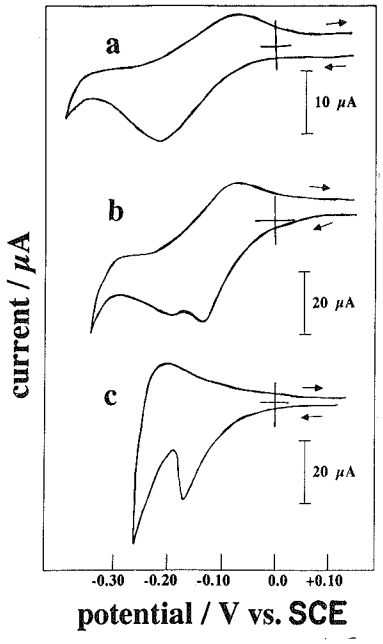

Fig. 2. Cyclic voltammetry (100 mV/s) of 5–10 mM $Ru(NH_3)_6^{3+}$ at an iridium oxide in contact with solutions at: a, pH 2; b, pH 1; c, pH 0. The positive potential limit in each case was +0.5 V. The oxide film was prepared by cycling 500 times at 5 V/s between −0.24 and +1.26 V vs. SCE.

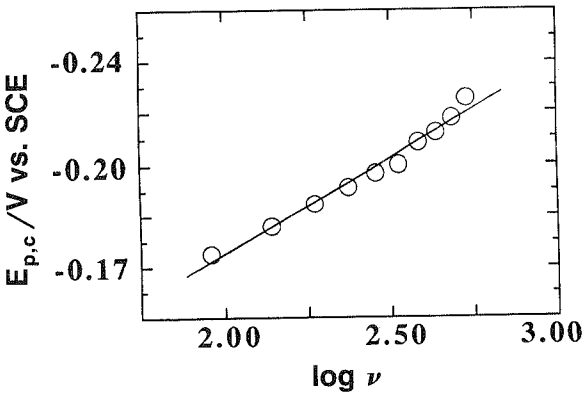

Fig. 3. Reductive peak potential vs. log sweep rate (mV/s) for $Ru(NH_3)_6^{3+}$ at an iridium oxide in 1.0 M H_2SO_4.

apparently indicating good film electrochemical conductivity in the vicinity of the $Ru(NH_3)_6^{3+/2+}$ formal potential (−250 mV). Figure 2b, obtained at pH 1, also shows a reversible response but shows additionally an apparently irreversible pre-peak (−190 mV). Finally, at pH 0 (Fig. 2c), only an irreversible peak is seen. The same experiment with $Ru(NH_3)_6^{2+}$ yields no electrochemical response, even though oxidation of the complex is thermodynamically favored over much of the potential range. Evidently, at this pH the film is behaving as a transient electrochemical rectifier (cathodic current flow only).

Follow-up experiments as a function of sweep rate ν show that the peak current (I_p) increases linearly with ν, indicating clearly that the reactant must be confined at the interface. Measurement of the peak potential as a function of sweep rate yields $\partial E_p/\partial \log \nu = -70$ mV/decade (slight curvature is evident; see Fig. 3).

As shown by Fig. 4, the magnitude of I_p is also strongly dependent on the positive reversal potential in the voltammetric scan. Comparison to Fig. 1 shows that the peak is seen only when the potential has previously been scanned through at least some portion of the Ir(III/IV) wave. Repetitive scan experiments indicate further that the positive potential excursion is required prior to every reductive scan for which the hexaammine ruthenium peak is to be observed. Figure 5 illustrates more quantitatively the relationship between $Ru(NH_3)_6^{3+}$ reactivity and Ir(III) oxidation. A plot of Q_{Ru} (the amount of reductive charge passed) and Q_{Ir} (the amount of film oxidation charge passed) is shown. The plot exhibits two linear regions, one with a (unitless) slope of 0.75 and the second with a slope of zero. Evidently only the most readily oxidizable iridium film sites (i.e. approximately the first 20%) are effective at binding $Ru(NH_3)_6^{3+}$, implying again that more than one type of metal-oxide site exists.

Returning to Fig. 4, it can be seen that not only the peak current but also the peak potential $E_{p,c}$ changes with the positive reversal potential for the voltammetric excursion. While the peak shift, and its apparent relationship to film loading,

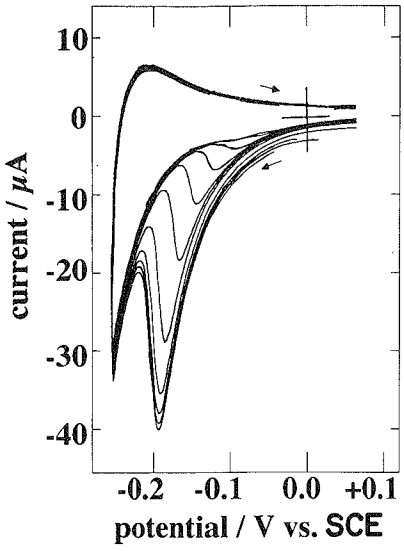

Fig. 4. Cyclic voltammograms (100 mV/s) for reduction of film-based $Ru(NH_3)_6^{3+}$ in 1 M H_2SO_4. The initial voltammogram (no Ru^{III} reduction current) features a positive reversal potential of +0.4 V. Subsequent voltammograms were obtained by progressively increasing the positive reversal potential by increments of +0.04 V, up to +0.84 V. The oxide film was prepared by cycling 500 times between −0.24 and +1.26 V.

might be interpreted in terms of uncompensated (film) resistance effects (recall that the oxide is electronically insulating in this region), at least one other interpretation is possible. Figure 6(a) shows that a plot of $E_{p,c}$ vs. log Q_{Ru} (i.e. film

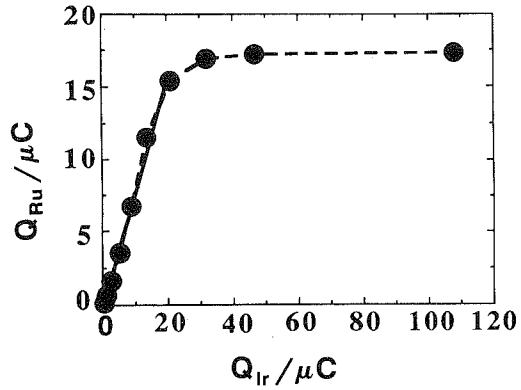

Fig. 5. Q_{Ru} vs. Q_{Ir} from cyclic voltammetry (100 mV/s) in 1.0 M H_2SO_4. The oxide film was grown by cycling 500 times between −0.24 and +1.26 V at 5 V/s. Charges were varied by increasing the positive potential limit in 0.04 V increments, beginning at +0.44 V ($Q_{Ir} < 2$ μC) and ending at +0.84 V ($Q_{Ir} = 108$ μC).

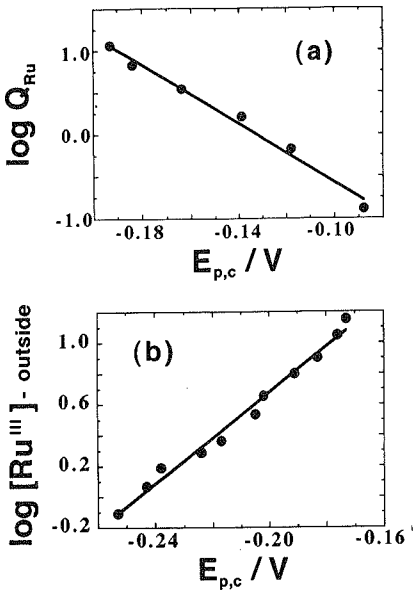

Fig. 6. Pseudo-Nernst plots of $E_{p,c}$ vs. $Ru(NH_3)_6^{3+}$ concentration, in 1 M H_2SO_4. (a) Variable internal concentration (Q_{Ru}, taken from Fig. 4) with fixed external concentration ([$Ru(NH_3)_6^{3+}$] = 7 mM). (b) Variable external $Ru(NH_3)_6^{3+}$ concentration with fixed internal concentration (Q_{Ru} = 16 μC). Both oxide films were prepared by cycling 500 times between −0.24 and +1.26 V at 5 V/s.

concentration) is linear with a slope of −57 mV. Given that the solution concentration of $Ru(NH_3)_6^{3+}$ is unchanging in these experiments, we ascribe the peak shifts tentatively to a Donnan potential (see below).

Finally, an attempt was made to determine the dependence of the extent of film loading (integrated rectification current, Q_{Ru}) on the concentration of $Ru(NH_3)_6^{3+}$ in solution. We observed no loading dependence between 1 and 14 mM; evidently the partition equilibrium lies completely to the left at all accessible concentrations. * As shown in Fig. 6(b), however, we did observe a systematic shift in $E_{p,c}$ vs. log [$Ru(NH_3)_6^{3+}$]. The relationship is linear with a pseudo-Nernstian slope of +67 mV (i.e. opposite in sign to that in Fig. 6(a)).

Control experiments with $[Ru(NH_3)_6](PF_6)_3$ in place of $[Ru(NH_3)_6](Cl)_3$ showed no changes in electrochemical response. On the other hand, controls with the electroinactive La^{3+} in place of the ammine complex showed, as expected, no electrochemical response in region 2.

* The lower solution concentration limit was determined by the extent of negative shift of $E_{p,c}$. Below 1 mM, $E_{p,c}$ overlapped severely with the current from hydrogen evolution.

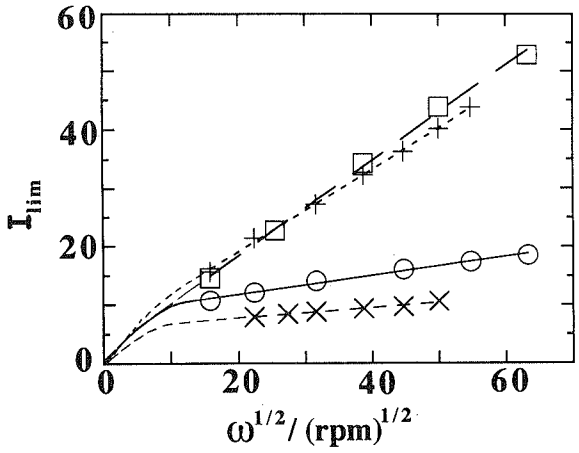

Fig. 7. Levich plots (I_{lim} vs. $\omega^{1/2}$) for the reduction of 10 mM $Ru(NH_3)_6^{3+}$ at a rotating iridium oxide film electrode. The pH values of the solutions were 9.7 (+), 7.0 (□), 3.8 (○) and 1.9 (×). No current was observable at pH 0. (The oxide film was grown with 900 cycles at 5 V/s between −0.24 and +1.26 V in 1 M H_2SO_4.)

Steady-state redox studies

To complement the transient studies, a series of steady-state (rotating disk voltammetry) studies was undertaken. Experiments at pH 0 showed that the film is completely blocked towards sustained $Ru(NH_3)_6^{3+}$ reduction. At pH 7, on the other hand, well-defined limiting currents (I_{lim}) are seen. Furthermore, the currents vary with the square-root of rotation rate (ω) and are equal (at all rotation rates) to the I_{lim} values seen at a nominally bare iridium metal surface. In view of these results it is tempting to ascribe the reactivity to some sort of residual conductivity in the reduced oxide at this pH. Consistent with that suggestion, the Ir(IV/III) wave (i.e. conductor/insulator transition) is in much closer proximity to the ruthenium couple at the higher pH. Additional experiments at intermediate pH values (Fig. 7), however, cast doubt on this interpretation. At pH 3.8, for example, Levich type behavior (linear I_{lim} vs. $\omega^{1/2}$ plot) is observed only up to rotation rates of about 100 rpm; at higher rates I_{lim} is significantly less than the extrapolated Levich current. Behavior of this type is usually indicative of slow chemical kinetics of some type. Indeed, the data in Fig. 7 can be satisfactorily fitted to Koutecky–Levich plots (I_{lim}^{-1} vs. $\omega^{-1/2}$), where the inverse intercepts of the plots provide measures of chemical reaction rates [28]. Analysis for $Ru(NH_3)_6^{3+}$ reduction yields progressively larger intercepts (i.e. smaller inverse intercepts, currents (I_{KL}) or rates) as the pH is increased.

Behavior of this type could conceivably still be consistent with pH-dependent changes in residual film conductivity. Another explanation, however, is that the oxide is electronically insulating in this potential range (as expected), but that it is

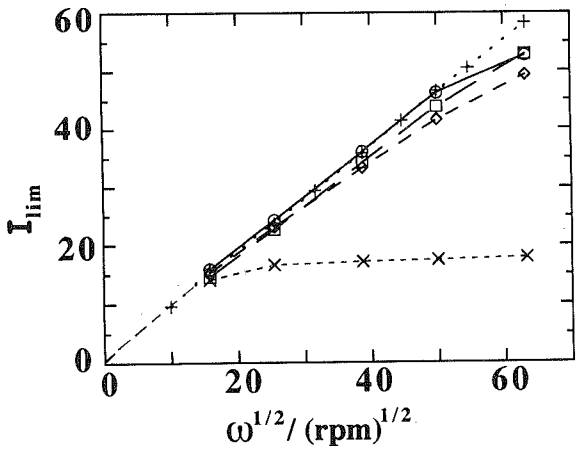

Fig. 8. Levich plots (I_{lim} vs. $\omega^{1/2}$) for the reduction of 10 mM $Ru(NH_3)_6^{3+}$ at a rotating iridium oxide film electrode at pH 7.0. Thickness of the oxide was varied by systematically varying the number of growth cycles (linear relationship) from 200 (+) to 400 (○), 900 (□), 1900 (◇) and 3400 (×). The cycling conditions are specified in Fig. 7.

permeable to the ruthenium cation. If reduction ultimately occurred rapidly at the underlying metal surface, then the rate-limiting chemical process would be diffusion through the oxide film [29,30]. Strong support for this interpretation is provided by Fig. 8 (I_{lim} vs. $\omega^{1/2}$) which shows that at a constant pH, the interfacial kinetics are significantly diminished by increasing the oxide-layer thickness.

Mechanistic interpretation

The preceding steady-state experiments demonstrate clearly that the insulating iridium (III) oxide film can function, at least at some pH values, as a cation-permeable membrane. Coupling of the Ir(III/IV) reaction (reaction (1)) to proton release and uptake suggests further that the film might display ion-exchange properties. * To rationalize the initial electrochemical findings (Figs. 2 and 4), therefore, we propose the following

$$3Ir^{III}(OH)_3(film) \rightarrow 3Ir^{IV}(O)(OH)_2(film) + 3H^+ + 3e^-(metal\ electrode) \quad (2)$$

$$3Ir^{IV}(O)(OH)_2(film) + 3e^-(metal\ electrode) + Ru(NH_3)_6^{3+}(soln.)$$
$$\rightarrow 3Ir^{III}(O)(OH)_2 \cdot Ru^{III}(NH_3)_6(film) \quad (3)$$

* Compelling evidence for non-protonic cation binding by electroactive iridium oxide (albeit, in non-aqueous solvents) has been reported by Glarum and Marshall [13] and by Pickup and Birss [31].

$$Ru(NH_3)_6^{3+}(film) + H^+(soln.) + e^-(metal\ electrode) \rightarrow Ru(NH_3)_6^{2+}(film) + H^+(film) \quad (4)$$

$$Ru(NH_3)_6^{2+}(film) + 2H^+(soln.) \rightarrow Ru(NH_3)_6^{2+}(soln.) + 2H^+(film) \quad (5)$$

Reactions (2) and (3) would clearly account qualitatively for the relationship (Fig. 4) between the extent of iridium oxidation and the extent of binding of $Ru(NH_3)_6^{3+}$. Quantitative agreement, on the other hand, would require a greater proton-to-electron ratio in reactions (2) and (3). For example, the alternative stoichiometry in reaction (6) would presumably lead to a $Q_{Ru}:Q_{Ir}$ ratio of 0.67, in better agreement with the reaction

$$Ir^{III}(OH)_2(H_2O)^+(film) \rightarrow Ir^{IV}(O)(OH_2)(film) + 2H^+ + e^-(metal\ electrode) \quad (6)$$

While we are unaware of any additional data which support a proton : electron ratio as large as 2, we note that Burke and Whelan [14] have obtained evidence (E_f vs. pH) for ratios as large as 1.5. For our experiments it is conceivable that an even higher stoichiometry occurs for the apparently unique sites (approx. 20% of the film total; see Fig. 1) involved in $Ru(NH_3)_6^{3+}$ uptake.

Returning to Scheme 1, reactions (3)–(5) imply the existence of a Donnan membrane potential which may be controlled, in part, by varying the ratio of $Ru(NH_3)_6^{3+}$ inside the film to $Ru(NH_3)_6^{3+}$ outside. The ability to vary these two concentrations independently (see Fig. 6 and text) would lead to both positive and negative concentration-induced potential shifts [32,33] (Fig. 6(a) and (b)) and to the following more general expression for $E_{p,c}$:

$$E_{p,c} = E_f(soln.) + \frac{RT}{nF}\ln\frac{\left[Ru(NH_3)_6^{3+}\right]outside}{\left[Ru(NH_3)_6^{3+}\right]inside} + constant \quad (7)$$

In eqn. (7) the constant would include factors responsible for the electrochemical irreversibility (see below) as well as concentration terms associated with other exchangeable ionic components of the electrolyte solution. Intuitively, eqn. (7) would seem to be the most applicable at fixed solution pH, conditions which are clearly met in our experiments.

Returning to Scheme 1, rapid irreversible kinetics for reaction (5) would account for the irreversible nature of reaction (4). If reaction (5) were extremely rapid, one might ultimately expect microscopic (i.e. interfacial) kinetic control of the overall electrochemical response via reaction (4). Ordinarily, the electrochemical kinetics of the $Ru(NH_3)_6^{3+/2+}$ couple would be regarded as too fast to measure by slow-sweep cyclic voltammetry. Note, however, that if reaction (5) were sufficiently rapid then $E_{p,c}$ for reaction (4) would be observed at significant underpotentials, where Tafel kinetics would necessarily lead to diminished rates for

electron transfer. While this "kinetic" interpretation is clearly speculative, it does account nicely for one remaining experimental observation: the very strong sweep-rate dependence of $E_{p,c}$. Assuming uncompensated film resistance effects can be neglected (a point still to be confirmed experimentally), standard voltammetry theory would predict a $\partial E_{p,c}/\partial \log \nu$ value of 59 mV/α, where α is the transfer coefficient [34]. Figure 3 suggests a potential dependence for α, with an average α value of 0.84. Note that a transfer coefficient in excess of 0.5 would be expected if the kinetics of reaction (4) were being monitored at potentials well positive of the true reversible, film-based potentials (as we have speculated above). Finally, the direction of reaction (5) as written would also be consistent with the blocking nature of the metal oxide film towards $Ru(NH_3)_6^{2+}$ oxidation in highly acidic solutions.

More generally, the pH-dependent blocking/permeability behavior in steady-state experiments can be rationalized by recognizing the inherent pH dependence of the composition of the iridium (III) coordination sphere. While the exact nature of the coordination environment is unclear, the pH dependence of the Ir(IV/III) redox potential (60–90 mV/pH unit) [2,14] implies a 1–1.5 proton equilibrium for Ir(III) over the available pH range; for example:

$$Ir(OH)_2O^- + H^+ \rightleftharpoons Ir(OH)_3 \quad (8)$$

or from reaction (6)

$$Ir(OH)_2O^- + 2H^+ \rightleftharpoons Ir(OH)_2(OH_2)^+ \quad (9)$$

Note that reaction (9) (but not reaction (8)) would impart pH-dependent cation exclusion (i.e. Donnan exclusion) characteristics to the electrode, as observed experimentally (see Fig. 7). Scheme 1, of course, provides a transient means for circumventing the Donnan exclusion effect, but would be ineffective in a steady-state experiment—again consistent with our observations. Finally, we suggest that while evidence for Scheme 1 is compelling only at lower pH values, the scheme (or at least reactions (2) and (3)) could well be operative at higher pH values, but might be unobservable by transient methods because of overlap with the permeation-based reduction reaction.

ACKNOWLEDGMENTS

We acknowledge helpful discussions with Prof. Jody Redepenning. We thank the Office of Naval Research for support of this work. JTH also acknowledges a Dreyfus Teacher-Scholar Award (1991–1996) and a fellowship from the Alfred P. Sloan Foundation (1990–1992).

REFERENCES

1 S. Gottesfeld and J.D.E. McIntyre, J. Electrochem. Soc., 126 (1979) 742.
2 G. Beni, C.E. Rice and J.L. Shay, J. Electrochem. Soc., 127 (1980) 1342.

3 S. Gottesfeld, J.D.E. McIntyre, G. Beni and J.L. Shay, Appl. Phys. Lett., 33 (1978) 208.
4 Y. Sato, M. Yanigida, H. Yamanaka and H. Tanigawa, J. Electrochem. Soc., 136 (1989) 863.
5 E.J. Frazer and R. Woods, J. Electroanal. Chem., 102 (1979) 127.
6 S. Hackwood, L.M. Schiavone, W.C. Dautremont-Smith and G. Beni, J. Electrochem. Soc., 128 (1981) 2569.
7 R. Kotz, H. Neff and S. Stucki, J. Electrochem. Soc., 131 (1984) 72.
8 S. Gottesfeld and S. Srinivasan, J. Electroanal. Chem., 86 (1978) 89.
9 P.G. Pickup and V.I. Birss, J. Electroanal. Chem., 240 (1988) 185.
10 P.G. Pickup and V.I. Birss, J. Electrochem. Soc., 135 (1988) 126.
11 P.G. Pickup and V.I. Birss, J. Electrochem. Soc., 135 (1988) 41.
12 P.G. Pickup and V.I. Birss, J. Electrochem. Chem., 220 (1987) 83.
13 S.H. Glarum and J.H. Marshall, J. Electrochem. Soc., 127 (1980) 1467.
14 L.D. Burke and D.P. Whelan, J. Electroanal. Chem., 124 (1981) 333.
15 L.D. Burke and D.P. Whelan, J. Electroanal. Chem., 162 (1984) 121.
16 L.D. Burke and D.P. Whelan, J. Electroanal. Chem., 175 (1984) 119.
17 B.E. Conway and J. Mozota, Electrochim. Acta, 28 (1983) 9.
18 S. Gottesfeld, J. Electrochem. Soc., 127 (1980) 122.
19 D. Cukman and M. Vukovic, J. Electroanal. Chem., 279 (1990) 283.
20 L.D. Burke and E.J.M. O'Sullivan, J. Electroanal. Chem., 117 (1981) 155.
21 S. Sisha, L. Amos, M.H. Schmidt and A.B. Bocarsly, J. Electroanal. Chem., 210 (1986) 323.
22 A. Capon and R. Parsons, J. Electroanal. Chem., 39 (1972) 275.
23 D.A.J. Rand and R. Woods, J. Electroanal. Chem., 55 (1974) 375.
24 D.N. Buckley and L.D. Burke, J. Chem. Soc. Faraday Trans. I, 71 (1975) 1447.
25 D.N. Buckley, L.D. Burke and J.K. Mulcahy, J. Chem. Soc. Faraday Trans. I, 72 (1976) 1896.
26 S.I. Nefedkin, N.V. Korovin, I.P. Gladkilch, G.N. Mansurov and O.A. Petrii, Sov. Electrochem., 24 (1988) 371.
27 S. Ardizzone, A. Carugati and S. Trasatti, J. Electroanal. Chem., 126 (1981) 371.
28 J. Koutecky and V.G. Levich, Zh. Fiz. Khim., 32 (1958) 1565.
29 T. Ikeda, R. Schmehl, P. Denisevich, K. Willman and R.W. Murray, J. Am. Chem. Soc., 104 (1982) 2683.
30 C.P. Andrieux and J.M. Saveant, J. Electroanal. Chem., 142 (1982) 1.
31 P.G. Pickup and V.I. Birss, J. Electroanal. Chem., 240 (1988) 171.
32 J. Redepenning and F.C. Anson, J. Phys. Chem., 91 (1987) 4549.
33 J. Redepenning, private communication.
34 R. Greef, R. Peat, L.M. Peter, D. Pletcher and J. Robinson, Instrumental Methods in Electrochemistry, Ellis Horwood, Chichester, 1985, Chapter 6.